ANL/CHM/PP--80544

BUCKYBALL MICROWAVE PLASMAS: FRAGMENTATION AND DIAMOND-FILM GROWTH†

Dieter M. Gruen,* Shengzhong Liu, Alan R. Krauss, and Xianzheng Pan
Materials Science/Chemistry Divisions
Argonne National Laboratory
9700 S. Cass Ave.
Argonne, IL 60439

DISCLAIMER

This report was prepared as an account of work sponsored by an agency of the United States Government. Neither the United States Government nor any agency thereof, nor any of their employees, makes any warranty, express or implied, or assumes any legal liability or responsibility for the accuracy, completeness, or usefulness of any information, apparatus, product, or process disclosed, or represents that its use would not infringe privately owned rights. Reference herein to any specific commercial product, process, or service by trade name, trademark, manufacturer, or otherwise does not necessarily constitute or imply its endorsement, recommendation, or favoring by the United States Government or any agency thereof. The views and opinions of authors expressed herein do not necessarily state or reflect those of the United States Government or any agency thereof.

August 1993

NOV 22 1993
OSTI

The submitted manuscript has been authored by a contractor of the U. S. Government under contract No. W-31-109-ENG-38. Accordingly, the U. S. Government retains a nonexclusive, royalty-free license to publish or reproduce the published form of this contribution, or allow others to do so, for U. S. Government purposes.

---

†Work supported by the U.S. Department of Energy, Division of Advanced Energy Projects, under Contract W-31-109-ENG-38.

MASTER

DISTRIBUTION OF THIS DOCUMENT IS UNLIMITED

BUCKYBALL MICROWAVE PLASMAS: FRAGMENTATION AND DIAMOND-FILM GROWTH

Dieter M. Gruen,* Shengzhong Liu, Alan R. Krauss, and Xianzheng Pan
Materials Science/Chemistry Divisions
Argonne National Laboratory
Argonne, IL 60439

ABSTRACT

Microwave discharges (2.45 GHz) have been generated in C_{60}-containing Ar. The gas mixtures were produced by flowing Ar over fullerene-containing soot at a variety of temperatures. Optical spectroscopy shows that the spectrum is dominated by the $d^3\Pi_g$-$a^3\Pi_u$ Swan bands of C_2 and particularly the $\Delta v = -2, -1, 0, +1$, and $+2$ sequences. These results give direct evidence that C_2 is in fact one of the products of C_{60} fragmentation brought about, at least in part, by collisionally induced dissociation (CID).

C_{60} has been used as a precursor in a plasma-enhanced chemical vapor deposition (PECVD) experiment to grow diamond-thin films. The films, grown in an Ar/H_2 gas mixture (0.14% carbon content, 100 Torr, 20 sccm Ar, 4 sccm H_2, 1500 W, 850°C substrate temperature), were characterized with SEM, XRD, and Raman spectroscopy. The growth rate was found to be ~0.6 μ/hr. Assuming a linear dependence on carbon concentration, a growth rate at least six times higher than commonly observed using methane as a precursor, would be predicted at a carbon content of 1% based on C_{60}. Energetic and mechanistic arguments are advanced to rationalize this result based on C_2 as the growth species.

Introduction

The behavior of C_{60} in collisions with surfaces, with other gaseous species, and with photons has been of interest since the earliest days of fullerene research (1) because the processes and mechanisms leading to fragmentation are of importance in achieving a full understanding of many of the fundamental properties of this molecule. An additional reason for interest in this topic is that C_{60} and the other fullerenes are unique, hydrogen-free, high vapor pressure, pure carbon species that are potential precursors in plasma chemistry and chemical vapor deposition. They are also potential sources of high intensity cluster beams for ion implantation and surface modification. The fragmentation and ionization processes that the fullerenes undergo will, to a large degree, determine the outcomes of such reactions.

The chief techniques in studying C_{60} fragmentation have generally involved mass spectrometric detection. Thus, the first systematic study of C_{60} photofragmentation observed only even-numbered clusters in the range C_{60} to C_{32} and concluded that these came about as a result of successive elimination of (undetected) neutral C_2 groups (2). Similar results have been obtained by a number of other research groups (3, 4, 5) and although the low mass fragments have always been assumed to be C_2 molecules, this conjecture still awaits experimental verification (6). The dissociating cluster ions have been treated by Klots (7) based on the statistical unimolecular decay of a canonical ensemble. With this approach, rate constants for fragmentation and for delayed electron emission have been deduced (8, 9).

In addition to photofragmentation, a number of studies had shown (10, 11) that highly accelerated C_{60}^+ and C_{70}^+ ions lose C_2 unimolecularly and presumably sequentially upon collisional activation (CA). Elimination of C_2 groups was also invoked to account for results of energetic collisions of C_{60} with gaseous H_2, D_2, Ar, or SF_6 (12, 13), with He or Xe (14), with Ne (15), with Li^+ and Na^+ (16), and with C^+ (17).

Energetic C_{60}^+ ion beam interactions with diamond surfaces were first modeled by Mowrey et al. in molecular dynamics simulations (18). Analysis of the trajectories gave detailed information about the dynamics of the collision process enabling energy thresholds for chemical *reactions with the surface and the distribution of products as a function of impact energy to be* calculated. At collision energies of 250 eV, the majority of the trajectories were found to be reactive in the sense that the C_2 fragment eliminated from the rebounding C_{58} remained attached to the surface. Experimental results in the reactive collision regime on HOPG graphite surfaces (19) show extensive fragmentation of C_{60}^+ in the scattered flux with a distribution of even-numbered fragments very similar to that found in photo as well as in gas phase CA fragmentation.

It appears then that, at least for clusters larger than C_{32}, fragmentation has been assumed to proceed almost exclusively by loss of neutral C_2 even though the C_2 fragment is energetically less favored than C_3 (20, 21). While entropy factors would enhance the loss of single carbon atoms, energetic considerations promote loss of the trimer. Again, the preferential loss of C_2 is in contradistinction to the abundance of the carbon species C, C_2, C_3, C_4, and C_5 in the equilibrium vapor of carbon at the sublimation temperature of 4100 K. These abundances are in the proportions 1, 2.8, 4.5, 0.35, and 0.5, respectively (22). Thus, the presumed evaporation of C_2 for C_n with $n > 32$ has been rationalized on the basis of free energy maximization in the overall fragmentation process leading to a compromise between thermodynamic stability and entropy considerations.

The dimer molecule, C_2, has not been seen as an abundant species in any of the studies involving mass spectrometric detection of the C_{60} fragmentation process. This situation is doubtless due to the high ionization potential of C_2 which is 12 eV. Instead, C atoms have recently been detected during multiphoton dissociation of laser-desorbed C_{60} (23). The (2+1) resonantly enhanced multiphoton ionization (REMPI) detection laser was also the dissociation laser in this experiment. Since the laser intensity (~ 1 GW/cm^2) was high enough to photodissociate C_2, it was not possible to conclude that the C-atoms were the primary dissociation products.

Fragmentation of C_{60} in Microwave Plasmas

It occurred to us that if a way could be found to produce high concentrations of C_{60} fragmentation products, particularly under conditions that would leave C_2 in electronically excited states below the dissociation threshold, direct detection of the C_2 fragment might be possible. Such conditions would be favored by the thermodynamic instability of C_{60} which would lead to ready sequential fragmentation once the special kinetic stability of the molecule has been breached. The potential of C_{60} as a precursor for diamond-film growth provided an additional stimulus for this work and will be discussed in the next section.

We attached a C_{60} sublimation source to a microwave (2.5 GHz) chamber (ASTeX, PDS-17). The experimental setup is shown schematically in Fig. 1. Fullerene-containing soot made either in our laboratory (24) or obtained from the MER Corporation was treated with methanol to remove most of the hydrocarbon constituents and placed in a gold container which in turn was situated in a quartz tube wound with nichrome wire. The chamber was evacuated and the soot heated to 250°C for 2 hrs. to remove the solvent, residual hydrocarbons, and adsorbed gases. To determine the rate of sublimation of C_{60}, the most volatile component in fullerene-containing soot, a silicon wafer was placed in front of the sublimation source while an argon flow was maintained in the quartz tube. With the source at 550°C, sufficient C_{60} was deposited in 1/2 hr. on the Si wafer so that the typical C_{60} IR absorption spectrum could be observed with good intensity (28,29). No features were seen in the I.R. spectrum that could not be attributed to C_{60}.

The silicon wafer was removed and, with fresh soot in the sublimation source, the temperature was again raised to 550°C. For initial experiments aimed at optical characterization of the plasma, a 500-W microwave discharge was initiated in 1 Torr Ar. A quartz fiberoptic cable viewed the discharge through a side window. The viewing region was 1-1.5 cm above the substrate. The light was transmitted to an Interactive Technology model 103 optical monochromator with 200 μm entrance and exit slit widths. The monochromator wavelength was stepped in increments of ≤ 2.3 Å with a dwell time of ≥ 100 msec/step. The detector was a Peltier-cooled photomultiplier tube operating in pulse counting mode, with a dark count rate of 20-30 cps. The Macintosh IIci control computer used custom software to provide a 100 msec gating pulse to the 32-bit National Instruments counter board located in the computer backplane.

A typical spectrum obtained from the intensely emerald-green plasma discharge is shown in Fig. 2. The spectrum is dominated by the $d^3\Pi_g$-$a^3\Pi_u$ Swan bands of C_2 (25,26), particularly the $\Delta v = -2, -1, 0, +1$, and $+2$ sequences (27). In other experiments, using either He as a carrier gas for the C_{60} or for a microwave discharge in C_{60} vapor, much less intense spectral features were observed.

It seems reasonable to conclude that very extensive fragmentation of C_{60} occurs in a microwave discharge sustained in 1 Torr Ar and that C_2 is the major observable product in an optical emission mode of detection. Thus, this experiment would appear to be the first direct evidence that C_2 is in fact the product of C_{60} fragmentation. The mechanism of fragmentation in such a microwave discharge is due to a number of different processes including collisional activation, charge exchange, electron collisions, direct microwave absorption by C_{60}, and energy transfer from metastable Ar atoms. Although free electrons probably play a role in sustaining the plasma and in the fragmentation process of C_{60} leading to ionic species and, in particular, to electronic and vibrationally excited C_2, absorption of microwave energy by argon, the accompanying excitation and ionization of argon atoms and the subsequent C_{60} fragmentation by collisional processes are also important. So far, cross sections for the various collisional processes involved in the production of C_2 molecules and in particular of excited C_2 molecules are not available, thus preventing the achievement of a quantitative understanding of the results. Since intense emission from excited Ar* atoms is also seen in the 6000-8000 Å region of the spectrum, high stationary concentrations of Ar in the metastable $^3P_2$ state at 11.55 eV lead in all likelihood to efficient energy transfer to C_{60} molecules.

It is known, particularly from the rate constants deduced from the unimolecular decay observed in photofragmentation (8), that 40-50 eV of internal energy must be acquired by the C_{60} molecule in order for decay rates to become appreciable. Four or more collisions of C_{60}

molecules with $^3P_2$ Ar atoms transferring energy by Penning processes could lead to C_{60} fragmentation. Since a low excitation energy (~ 2.4 eV) is required to observe Swan band emission, it is possible that the C_{60} fragmentation process leads directly to C_2*. Alternatively, C_2 is excited to C_2* in a subsequent collision with Ar*. Much must be learned about the energetics of the fragments and the various ion and neutral constituents of the plasma before a reasonably detailed picture of the mechanism of the microwave initiated fragmentation process of C_{60} emerges. We are beginning to conduct experiments to measure the plasma constituents mass spectrometrically in order further to elucidate the fragmentation phenomena.

Although we have not yet done a detailed analysis of the Swan bands as has been done by Rohlfing, for example, (27), in studies of C_2 produced by laser desorption of graphite, it is of interest to compare our data on the $\Delta v = -1$ sequence with those obtained in that work (27). The close similarity in the relative intensities of the peaks in that sequence shown in our Fig. 2 and in Rohlfing's Fig. 3 argues for similar vibrational ($T_{vib} \sim 10^4$ K) and rotational temperatures ($T_{rot} \sim 10^3$ K) in the two experiments. While Rohlfing argued that his electronically excited C_2 from the laser plume was probably nascent and produced via multiphoton dissociation of larger carbon clusters and particles, we have very strong evidence that our C_2 in fact comes from the fragmentation of C_{60} as discussed above.

To strengthen this conclusion, we performed the following experiment. Emission spectra were obtained as described previously but as a function of sublimator temperature. The Swan band emission intensities were found to increase as a function of temperature as shown in Fig. 3, Curve A. Under saturation conditions of the Ar carrier gas, the emission intensities should follow the vapor pressure curve of C_{60} (Fig. 3, Curve B). A log plot clearly shows that the carrier gas is far from saturated with the equilibrium C_{60} pressure. The C_2 concentration in the plasma increases with temperature due to increased C_{60} volatility, thus demonstrating that the C_2 emission is not due to a minor constituent or to carbon particles transported into the plasma. Continuation of this experiment for several hours at sublimator temperatures of 550°C results in depletion of C_{60} and presumably higher fullerenes as evidenced by decreasing Swan band intensities. After such a prolonged experiment, lowering the temperature to 500°C results in emission spectra with intensities less by a factor of 10 than those obtained with a fresh batch of soot.

Additional experiments were performed as a function of microwave power to gain insight into the fragmentation efficiency. In the range 500-1200 W, neither the absolute intensities nor the intensity ratios of the different Swan band sequences were significantly affected. One is tempted to conclude that fragmentation is complete even at 500 W, the lowest microwave power achievable in our system. We are currently conducting experiments that will allow us to go lower in microwave power in order to study the power dependence of the C_2 emission in detail.

Diamond-Film Growth Using C_{60} as a Precursor

The extensive fragmentation of C_{60} to C_2 in an argon plasma observed in the course of the work reported here led us to speculate on the potential of using C_{60} as a precursor to plasma-enhanced chemical vapor deposition (PECVD) of diamond films. The chemical vapor deposition of diamond is now an established technology (30). The various processes which have been elaborated up to now involve in the main hydrocarbon gases as precursors. A frequently discussed growth mechanism involves the $CH_3•$ radical as the principal growth species (31), particularly when methane is used as the precursor gas. More recently, C_2H_2 has been invoked as the growth species (32,33) when acetylene is used as the precursor (34). Both the $CH_3•$ and C_2H_2 based mechanisms involve the reaction of atomic hydrogen both with surface hydrogens and with the respective hydrocarbon species adsorbed on the growing surface. Such hydrogen abstraction reactions are required in the case of hydrogen-containing growth species in order for carbon to be incorporated into the diamond lattice. It could turn out that using the C_2 molecule as a growth species results in more rapid incorporation of carbon and therefore to higher diamond-film growth rates.

The experimentally determined adsorption energy of C_2 on a graphite surface is very high, 815 kJ (35) compared to model calculations of approximately 50 kJ for C_2H_2 adsorbing on a $C_{22}H_{27}•$ template simulating diamond (36). Although these two situations are not strictly comparable, it is entirely likely that C_2 can insert directly into the C-H bonds of a hydrogen terminated diamond surface. To explore the energetics of such a mechanism for diamond growth, we consider the reaction

$$C_2(^1\Sigma_g^+) + CH_4 \rightarrow H_3CHCC \rightarrow H_3CCCH \qquad (1)$$

as a simple and certainly much oversimplified model for addition of C_2 to a diamond surface. The first step corresponds to insertion of singlet C_2 into the C-H bond. The second step corresponds to migration of the hydrogen to the terminal carbon. The energy for the overall reaction has been calculated using G2 theory (37,38), a method based on ab initio molecular orbital theory for the calculation of reaction energies accurate to ± 2 kcal/mol. The energy, ΔE_0, for reaction

$$C_2(^1\Sigma_g^+) + CH_4 \rightarrow H_3CCCH \qquad (2)$$

is -128.3 kcal/mol from G2 theory indicating that formation of propyne, H_3CCCH, is very favorable compared to C_2 and CH_4. The energy of 1-propeneylidene, $H_3CHC{=}\,C{:}$, has not been determined yet at the G2 level of theory. At a lower level of theory, HF/3-21G, it is 43.4 kcal/mol less stable than propyne.

Preliminary results (38) from low level calculations (HF/3-21G) of the potential energy surface suggest little or no barrier for the first step of reaction (1), i.e., insertion of C_2 into a CH bond of methane to form H_3CHCC. The barrier for isomerization of H_3CHCC to H_3CCCH, the seond step in reaction (1), is about 31 kcal/mol at the HF/3-21G level. Generally, these types of barriers are reduced at higher levels of theory. With C_2 as the growth species, the 13-step mechanism proposed by Belton and Harris (33) could be reformulated as a 5-step mechanism with the first two steps being successive C_2 insertion reactions. The remaining three steps would then be identical to steps 11-13 of Belton and Harris (33). The 5-step C_2 mechanism strongly reduces the requirement for hydrogen abstraction reactions and this, coupled with rapid C_2 insertions, could lead to improved growth kinetics (39).

In order to test the supposition that C_{60} can be a precursor to diamond-film growth, the following experiment was performed. Fullerene-containing soot was placed in the experimental set-up shown in Fig. 1. With the temperature of the soot at 550°C, an Ar/H_2 mixture (20 sccm Ar, 4 sccm H_2) was passed through the sublimator into the plasma chamber while maintaining a total pressure of 100 Torr. A 3"-diameter single-crystal silicon disc which had been mechanically treated with 0.1 μ diamond powder was placed on a graphite holder and maintained at 850°C during the experiment. A 1500-W microwave discharge was maintained in the gas mixture during a 16-hr deposition. Optical emission measurement showed intense C_2 Swan band emission, as well as intense H_α and H_β but relatively much weaker Ar emission lines. The Si substrate was examined after the deposition using SEM, XRD, and Raman spectroscopic techniques. SEM images of a portion of the substrate (Fig. 4) at 9,500 magnification shows micron-sized particles which appear to be polycrystalline aggregates. The film thickness is ~10 μ giving an estimated growth rate of ~0.6 μ/hr (Fig. 5). An x-ray diffraction pattern (Phillips powder diffractometer with Cu K_α) of the film is shown in Fig. 6. Characteristic <111>, <220>, and <311> diamond reflections are obtained from the same portion of the substrate used for the SEM examination.

A Raman spectrum (Fig. 7) was obtained using a SPEX model 1403 double monochromator fitted with a photomultiplier tube detector. Data acquisition was by a SPEX Scamp controller. The 514.5 nm line of a coherent model Innova 300 Ar^+ laser was used for sample excitation at a power level of 100 mW. The spectrum has the characteristic diamond peak at 1334 cm^{-1} and a broad feature with a maximum at ~1530 cm^{-1} which is usually attributed to nondiamond carbon phases. The peak shapes and relative intensities are reminiscent of diamond grown from 1% CH_4 in H_2 mixtures. (See Fig. 1 in Ref. 40) The discussion given by Yarbrough and Messier (40) of the Raman spectrum taken on their polycrystalline diamond film is very relevant to our work. The position and intensity of the broad peak depends on a variety of factors and is still a subject of lively controversy. Based on the broad peaks in our x-ray diffraction pattern and the cauliflower-like features observed in SEM, we assign the ~1530 cm^{-1} feature to a highly disordered C phase, possibly diamond-like C (DLC) (41). Additional arguments for this assignment are that (1) the peak position falls into the range of DLC, 1540 ± 20 cm^{-1} (42), and (2) no evidence for a graphitic phase was found in the x-ray diffraction pattern.

A very crude assessment of growth rate using C_{60} rather than CH_4 as a precursor can be made. The vapor pressure of C_{60} at 550°C is 2.32 mTorr (28) and therefore, assuming saturation, the Ar/H_2 gas mixture contained 0.14% C. For the ASTeX PDS-17 system [see Standard Operating Procedure for the Applied Science and Technology, Inc. Diamond Deposition Source (March 18, 1992)], a 1% CH_4 in H_2 mixture at ~100 Torr and ~ 1500 W gives a growth rate of 0.75 μ/hr. If one assumes that the growth rate is linearly dependent on carbon content in the range 0.14-1% carbon, one would expect growth rates at least six times higher with C_{60} than with standard CH_4/H_2 mixtures. Since, as previously discussed, the carrier gas is not saturated with C_{60} vapor, this calculated growth rate should be regarded as a lower limit. We are planning experiments at sublimator temperatures higher than 550°C to investigate the effect of higher C_{60} vapor pressures and therefore higher carbon concentrations on diamond-film growth rates.

Conclusion

The generation of microwave plasmas in C_{60}/Ar and C_{60}/Ar/H_2 mixtures results in molecular emission spectra dominated by the Swan bands (d $^3\Pi_g$-a$^3\Pi_u$) of C_2. This observation provides strong evidence for the correctness of the assumption frequently made in a wide variety of studies that C_{60} fragmentation proceeds via the elimination of C_2 groups. Collisionally induced dissociation of C_{60} in argon plasmas could be an effective mechanism for C_2 production. Microwave plasmas, therefore, appear to be efficient sources for this highly reactive molecule. Emission spectroscopy, which has been used in the present study to identify C_2, is not well suited to quantitative measurements of the concentration of the molecule in the plasma. Therefore, a plasma sampling system involving time-of-flight mass spectrometric detection has been set up in our laboratory to measure C_2 levels and to identify other carbon-containing species that may be present in the plasma.

The copious amounts of C_2 provided by the microwave plasma dissociation of C_{60} present a unique opportunity to explore the potential role of the C_2 molecule as a growth species in the deposition of diamond films. Our work has now demonstrated that C_{60} can act as a precursor for diamond growth rather than the previously demonstrated nucleation of diamond on C_{60} films (43). We propose that C_2 is in fact the principal growth species under the conditions of our experiment. Energetic and mechanistic arguments are advanced, based on ab initio calculations of the reaction of C_2 with CH_4, to support the notion that C_2 can insert directly into C-H bonds terminating the surface of diamond, thus reducing the need for hydrogen abstraction reactions required for hydrocarbon precursors. The observed increased growth rate of the diamond film could be a direct result of removing some of the kinetic barriers to growth encountered with other growth species.

Acknowledgements

We wish to acknowledge helpful discussions with Dr. Keith Lykke. Dr. Larry Curtiss kindly made available to us results of his preliminary ab initio calculations. We thank Drs. Carlos Melendres for allowing us to use his Raman spectrometer and Ben Tani for the x-ray results.

References

1. For a review of this topic, see D. M. Gruen, *Nucl. Instr. and Methods,* Physics Research B78, 118 (1993).

2. S. C. O'Brien, J. R. Heath, R. F. Curl, R. E. Smalley, *J. Chem. Phys.* **88**, 220 (1988).

3. S. W. McElvany, J. H. Callahan, *J. Phys. Chem.* 95, 6186 (1991); K. R. Lykke, M. J. Pellin, P. Wurz, D. M. Gruen, J. E. Hunt, M. R. Wasielewski, *Mater. Res. Soc. Proc.* **206**, 679 (1991).

4. P. Wurz, K. R. Lykke, M. J. Pellin, D. M. Gruen, *J. Appl. Phys.* **70**, 6647 (1991).

5. E. E. B. Campbell, G. Ulmer, I. V. Hertel, *Phys. Rev. Lett.* **67**, 1986 (1991).

6. P. P. Radi, T. L. Bunn, P. R. Kemper, M. E. Malchan, M. T. Bowers, *J. Chem. Phys.* **88**, 2809 (1988).

7. C. E. Klots, *Z. Phys. D.* **21**, 335 (1991); *Chem. Phys. Lett.* **186**, 73 (1991); *J. Chem. Phys.* **90**, 4470 (1989); *Z. Phys. D.* **20**, 105 (1991); *Acc. Chem. Res.* **21**, 16 (1988); *J. Phys. Chem.* **92**, 5864 (1988).

8. P. Wurz, K. Lykke, *J. Chem. Phys.* **95**, 7008 (1991).

9. P. Wurz, K. R. Lykke, *J. Phy. Chem.* **96**, 10129 (1992).

10. P. P. Radi, M. T. Hsu, J. Brodbelt-Lustig, M. Kincon, M. T. Bowers, *J. Chem. Phys.* **92**, 4817 (1990); A. B. Young, L. M. Cousins, A. G. Harrison, *Rapid Commun. Mass Spectrom.* 5, 226 (1991); D. R. Luffer, K. H. Schram, *Rapid Commun. Mass Spectrom*. **4**, 552 (1990); P. P. Radi, M. T. Hsu, M. E. Rincon, P. R. Kemper, M. T. Bowers, *Chem. Phys. Lett.* **174**, 223 (1990); C. Lifshitz, M. Iraqi, T. Peres, J. E. Fischer, *Int. J. Mass. Spectrom. Ion Processes,* in press; C. Lifshitz, M. Iraqi, T. Peres, J. E. Fischer, *Rapid Comm. Mass Spectrom.* **5**, 238 (1991); D. Schröder, D. Sülzle, *J. Chem. Phys.* **94**, 6933 (1991); R. J. Doyle, Jr., M. M. Ross, *J. Phys. Chem.*, in press.

11. Reviews: R. G. Cooks, Ed., Collision Spectroscopy, Plenum, New York (1978); K. Levsen, H. Schwarz, *Mass Spectrom. Rev.* **2**, 77 (1983); J. Bordas-Nagy, K. R. Jennings, *Inst. J. Mass Spectrom. Ion Processes* **100**, 105 (1990).

12. T. Weiske, D. K. Böhme, J. Hrusak, W. Krätschmer, H. Schwarz, *Angew. Chem. Int.*, Ed. Engl. 30, 884 (1991).

13. T. Weiske, J. Hrusak, D. Böhme, H. Schwarz, *Chem. Phys. Lett.* **186**, 459 (1991).

14. M. M. Ross, J. H. Callahan, *J. Phys. Chem.* **95**, 5720 (1991).

15. Z. Wan, J. F. Christian, S. L. Anderson, *J. Chem. Phys.* **96**, 3344 (1992).

16. Z. Wan, J. F. Christian, S. L. Anderson, *J. Chem. Phys.*, in press.

17. J. F. Christian, Z. Wan, S. L. Anderson, *J. Phys. Chem.* **96**, 3574 (1992).

18. R. C. Mowrey, D. W. Brenner, B. I. Dunlap, J. W. Mintwire, C. T. White, *Mater. Res. Soc. Symp. Proc.* **206**, 357 (1992); *J. Phys. Chem.* **95**, 7138 (1991).

19. H.-G. Busmann, Th. Lill, I. V. Hertel, *Chem. Phys. Lett.* **187**, 459 (1991).

20. K. Raghavachari, S. Binkley, *J. Chem. Phys.* **87**, 2191 (1987).

21. K. S. Pitzer, E. Clementi, *J. Am. Chem. Soc.* 21, 4477 (1959); D. W. Ewing, G. V. Pfeiffer, *Chem. Phys. Lett.* **86**, 365 (1982); K. Raghavachari, R. A. Whiteside, J. A. Pople, *J. Chem. Phys.* **85**, 6623 (1986); S. J. Strickler, K. S. Pitzer, in *Molecular Orbitals in Chemistry,* edited by B. Pullmann and P. O. Löwdin (Academic, New York, 1964), p. 281.

22. J. Drowart, R. P. Burns, G. De Maria, M. J. Inghram, *J. Chem. Phys.* **31**, 1131 (1959).

23. K. R. Lykke, P. Wurz, D. H. Parker, M. J. Pellin, *Appl. Optics* **32**, 857 (1993).

24. D. H. Parker, P. Wurz, K. Chatterjee, K. R. Lykke, J. E. Hunt, M. J. Pellin, J. C. Hemminger, D. M. Gruen, and L. M. Stock, *J. Am. Chem. Soc.* **113**, 20 (1991).

25. K. P. Huber and G. Herzberg, *Molecular Spectra and Molecular Structure IV. Constants of Diatomic Molecules,* Von Nortrand Reinhold, New York, 1979, Appendix IV.

26. W. Weltner, Jr. and R. J. Van Zee, *Chem. Rev.* **89**, 1713 (1989).

27. E. A. Rohlfing, J. Chem. Phys. **89**, 6103 (1988).

28. J. Abrefah, D. R. Olander, M. Balooch, and W. J. Siekhaus, *Appl. Phys. Lett.* **60**, 1313 (1992).

29. R. Meilunas, R. P. H. Chang, S. Liu, and M. Kappes, J. Appl. Phys. **70**, 5128 (1991).

30. Proceedings of the Third International Conference on the New Diamond Science and Technology (ICNDST-3), Elsevier 1993, P. K. Bachmann, A. T. Collins, M. Seal, Editors.

31. For a recent review, see J. E. Butler and R. C. Woodin, Phil. Trans. R. Soc. London **A342**, 209 (1993).

32. M. Frenklach and K. E. Spear, J. Mater. Res. **3**, 133 (1988).

33. D. N. Belton and S. J. Harris, J. Chem. Phys. **96**, 2371 (1992).

34. S. J. Harris and L. R. Martin, J. Mater. Res. **5**, 2313 (1990).

35. R. J. Thorn and G. H. Winslow, J. Chem. Phys. **26**, 186 (1957).

36. K. Larsson, S. Lunell, and J.-O. Carlsson, Diamond and Related Materials 2, 949 (1993).

37. L. A. Curtiss, K. Raghavachari, G. W. Trucks, and J. A. Pople, J. Chem. Phys. **94**, 7221 (1991).

38. Some of the energies used to obtain the reaction energies and barriers reported here were obtained from the Carnegie-Mellon, University Quantum Chemistry Archive.

39. The C_2 mechanism proposed here is being further investigated using G2 theory in collaboration with Dr. Larry Curtiss, Argonne National Laboratory.

40. W. A. Yarbrough and R. Messier, Science **247**, 688 (1990).

41. C. Wild, N. Herres, J. Wagner, P. Koidl, T. R. Anthony, in Proceedings of the First International Symposium on Diamond and Diamond-like Films, J. P. Dismukes et al., Eds. (The Electrochemical Society, Pennington, NJ, 1989), pp. 283-295.

42. P. V. Huang, Diamond and Related Materials 1, 33 (1991).

43. R. Meilunas, R. P. H. Chang, S. Liu, and M. Kappes, Appl. Phys. Lett. 59, 3461 (1991).

Fig. 1 - Schematic of a 2.5 GHz microwave plasma deposition chamber with an attached sublimation source (inset) consisting of a quartz tube upon which is wound a nichrome heating element. Fullerene-containing soot is wrapped inside a gold boat to prevent pickup by the carrier gas. An orifice in the boat is directed toward the plasma chamber where the fullerene vapor mixes with the carrier gas. The RF-induction heated substrate stage holds a silicon disc. A fiber optic is fastened to the quartz window, viewing the plasma 1-1.5 cm above the substrate stage.

Fig. 2 - Swan band emission of C_2 produced by fragmentation of C_{60} in 1 Torr argon carrier gas excited by a 500 W 2.45 GHz microwave plasma.

Fig. 3 - Vapor pressure of C_{60} (righthand scale. Data taken from Ref. 28.) Integrated intensity of the $\Delta v = 0$ band from C_2 emission as a function of sublimator temperature (lefthand scale).

Fig. 4 - SEM image of diamond film grown on a Si substrate at 9,500 magnification from a $C_{60}/Ar/H_2$ microwave plasma.

Fig. 5 - Cross-sectional SEM image of the diamond film at 2000 magnification.

Fig. 6 - XRD scan of the same deposition region on the Si substrate subjected to SEM examination. Note the prominent <111> peak.

Fig. 7 - Raman spectrum of diamond film grown from a $C_{60}/Ar/H_2$ mixture.

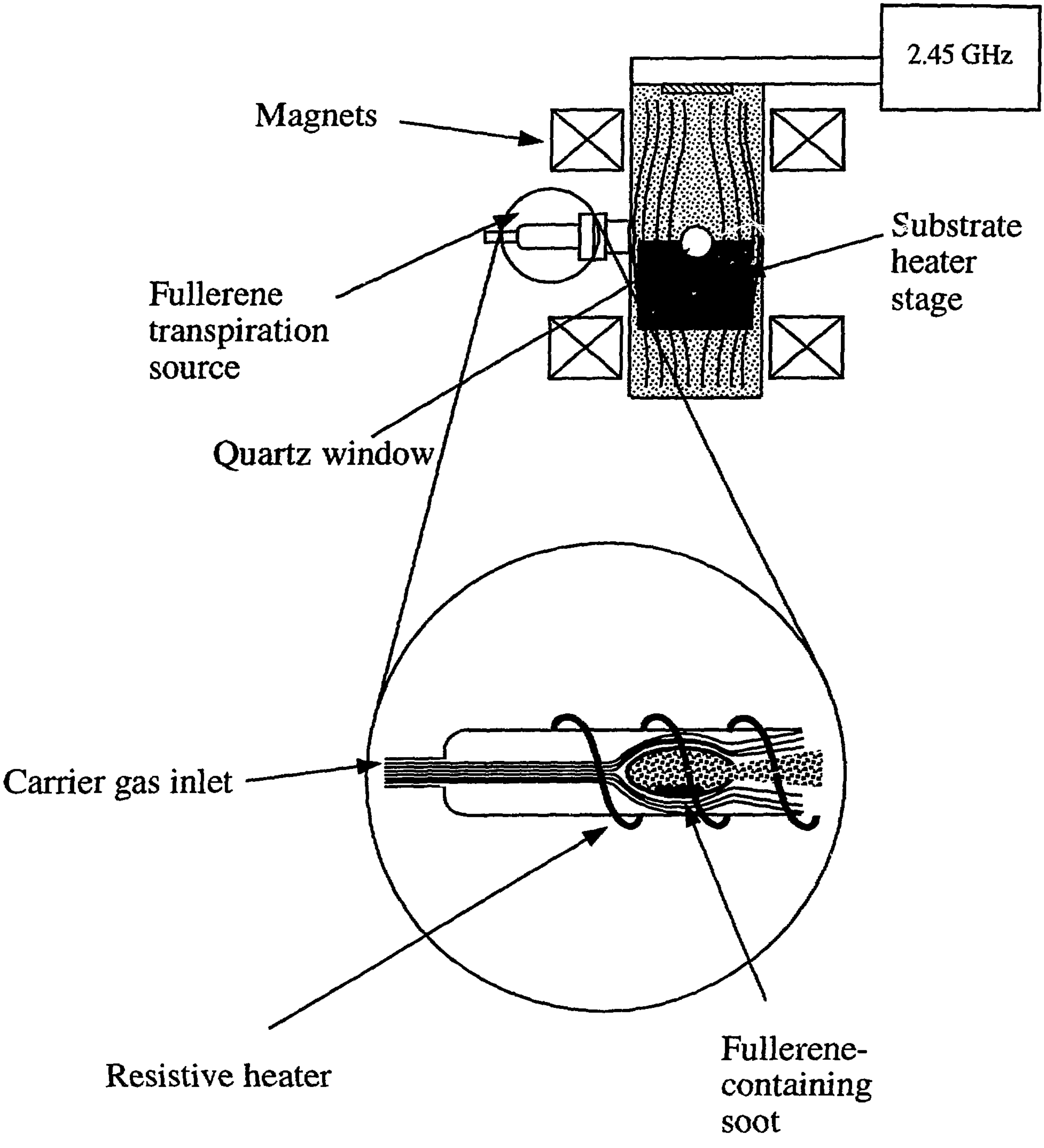
2.45 GHz
Magnets
Substrate heater stage
Fullerene transpiration source
Quartz window
Carrier gas inlet
Resistive heater
Fullerene-containing soot

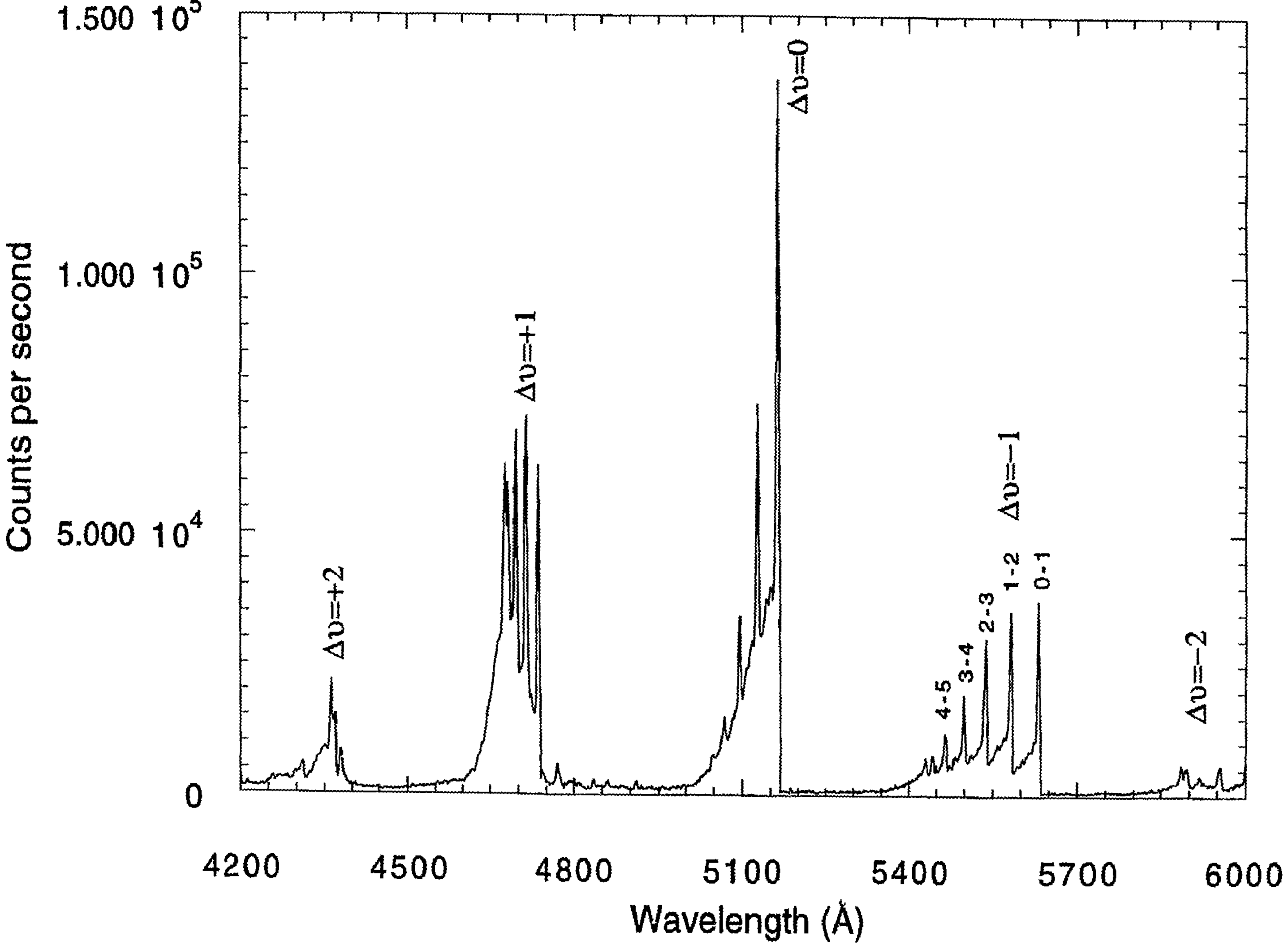

1.500 10^5
1.000 10^5
5.000 10^4
0
Counts per second
4200
4500
4800
5100
5400
5700
6000
Wavelength (Å)
Δυ=+2
Δυ=+1
Δυ=0
4-5
3-4
2-3
1-2
0-1
Δυ=−1
Δυ=−2

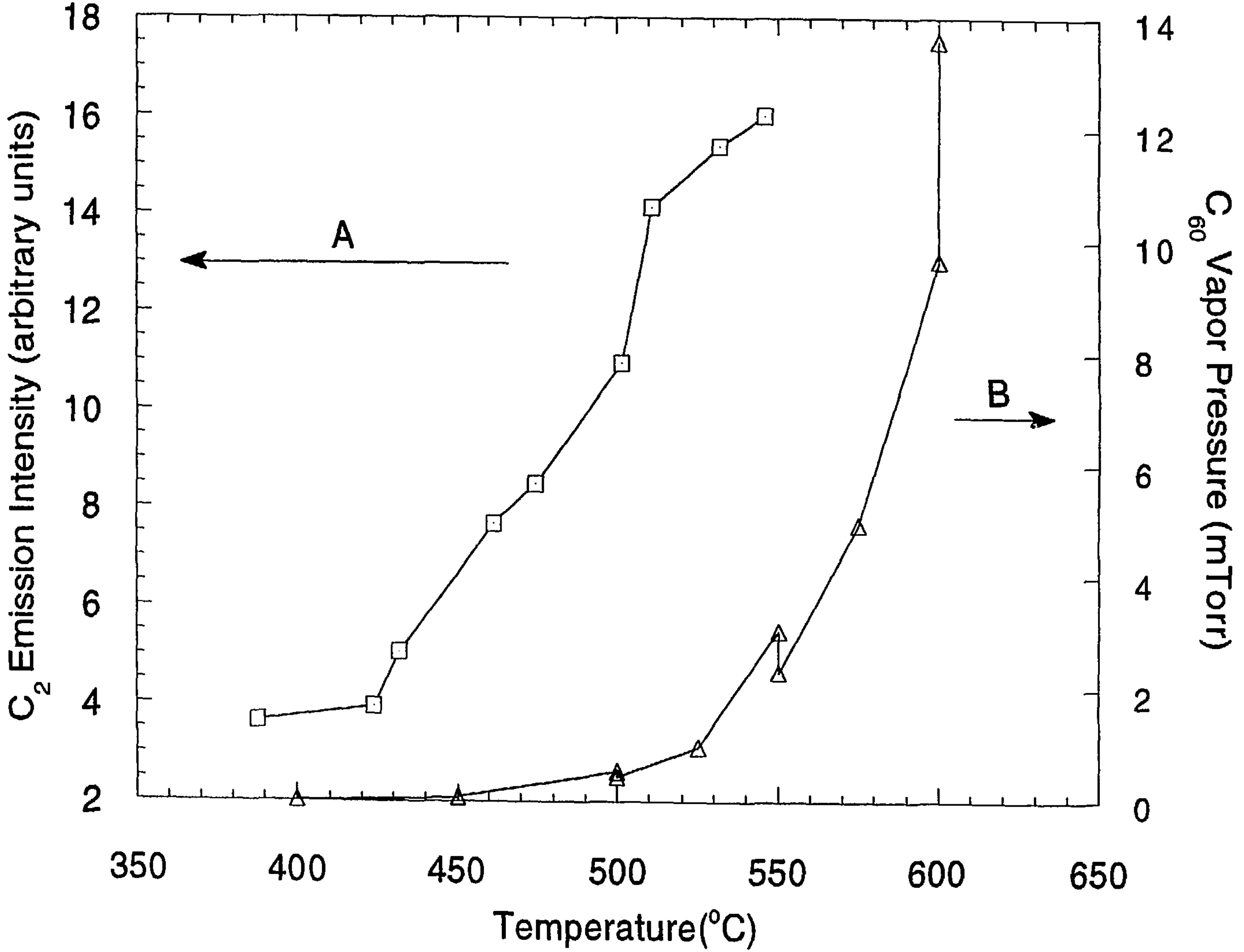
C$_2$ Emission Intensity (arbitrary units)
18
16
14
12
10
8
6
4
2
A
B
C$_{60}$ Vapor Pressure (mTorr)
14
12
10
8
6
4
2
0
350
400
450
500
550
600
650
Temperature(°C)

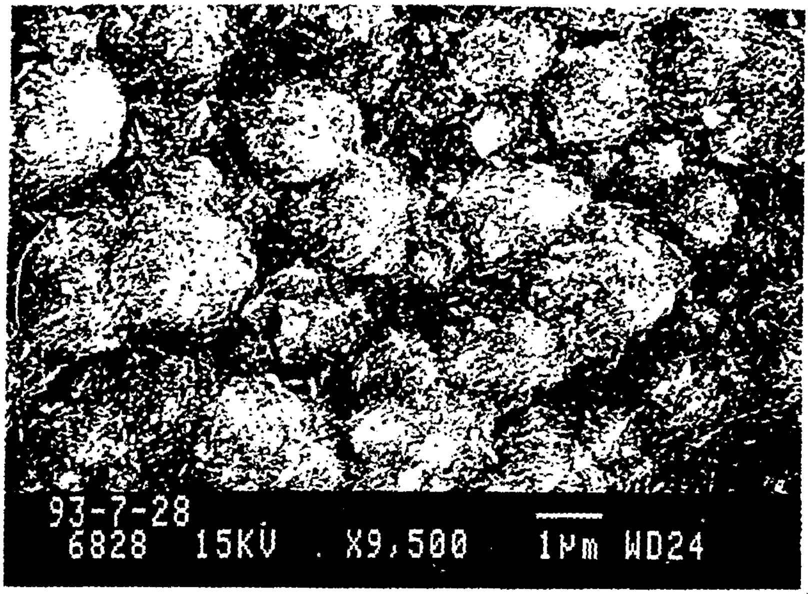
93-7-28
6828 15KV X9,500 1μm WD24

Fig. 4

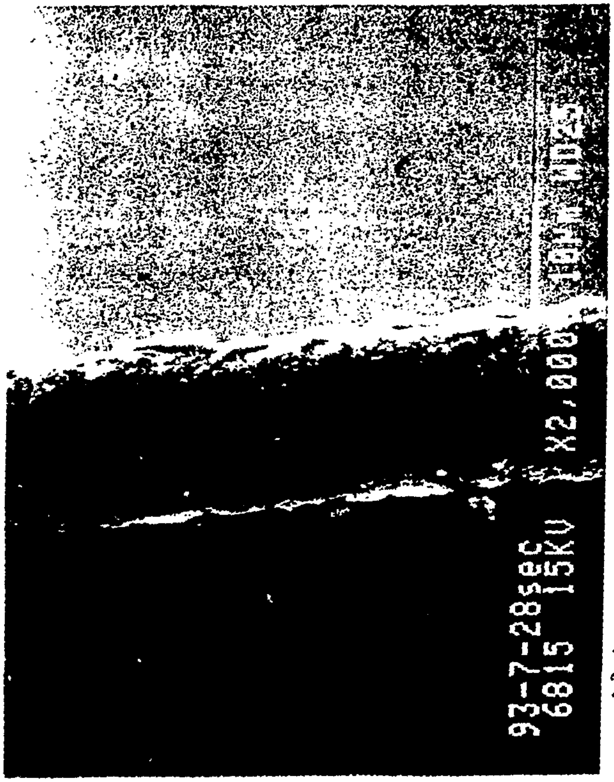
93-7-28sec
6815 15KV X2,000 10μm WD25

10μ

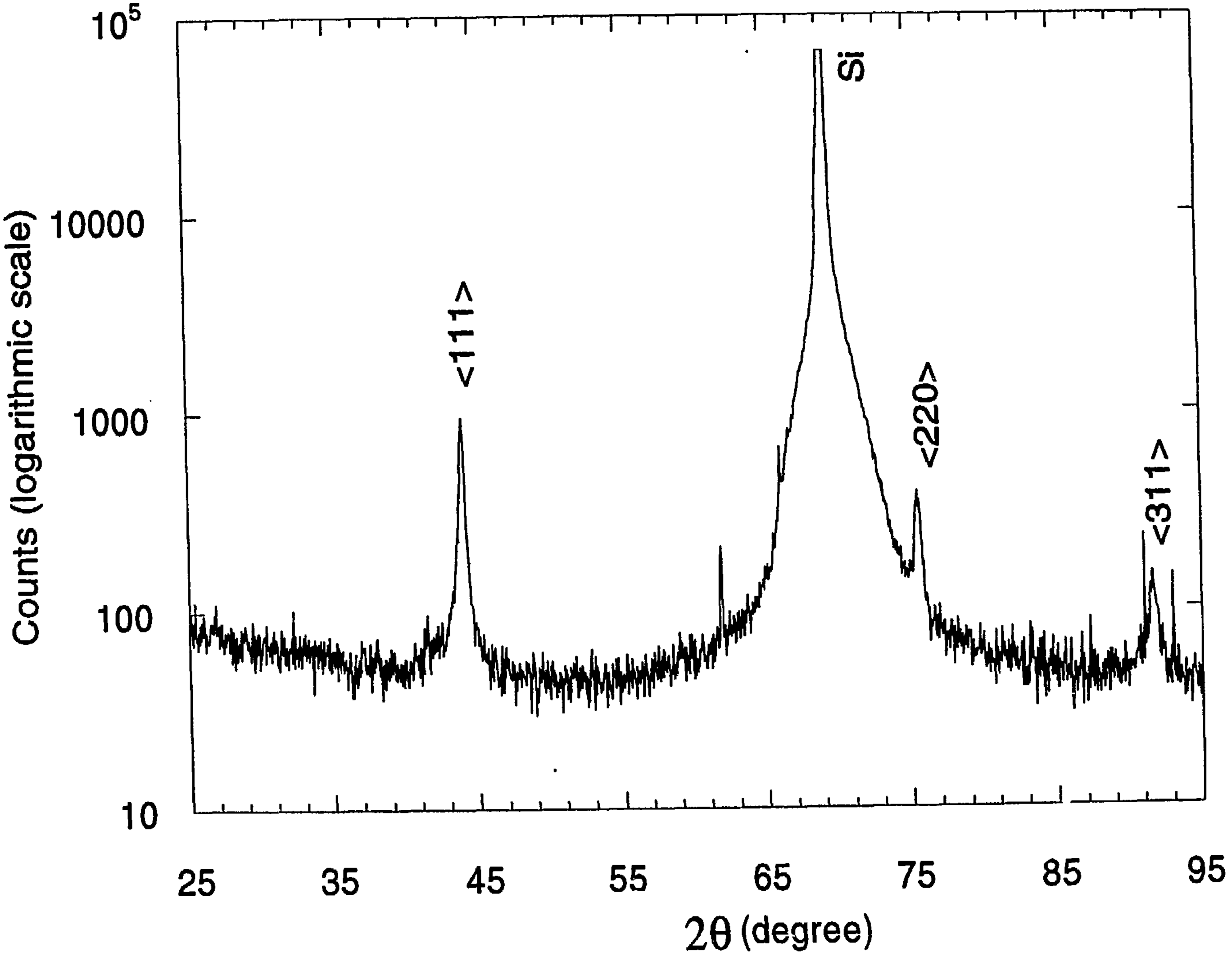
10^5
10000
1000
100
10
Counts (logarithmic scale)
25
35
45
55
65
75
85
95
2θ (degree)
<111>
Si
<220>
<311>

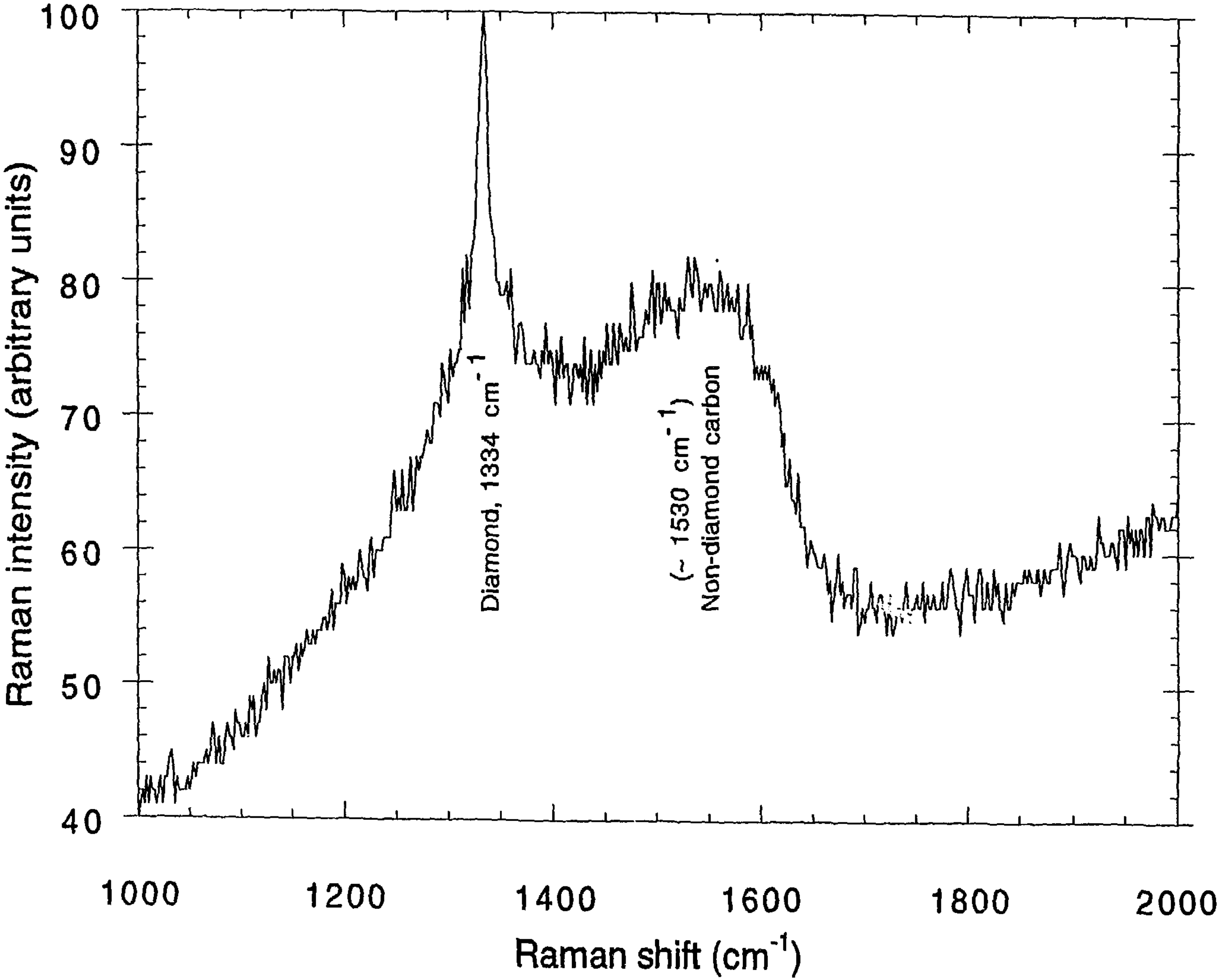
100
90
80
70
60
50
40
Raman intensity (arbitrary units)
Diamond, 1334 cm-1
(~ 1530 cm-1)
Non-diamond carbon
1000
1200
1400
1600
1800
2000
Raman shift (cm-1)